Minority-carrier recombination in *p*-InP single crystals

Y. Rosenwaks, I. Tsimberova, and H. Gero
Department of Physical Electronics, Faculty of Engineering, Tel Aviv University, Ramat-Aviv 69978, Israel

M. Molotskii
The Wolfson Materials Research Center, Tel Aviv University, Ramat-Aviv 69978, Israel

(Received 8 April 2002; revised manuscript received 15 October 2002; published 30 September 2003)

We present a comprehensive and systematic study of minority-carrier lifetime and recombination mechanisms in *p*-InP single crystals. The study is based on steady state and time-resolved photoluminescence measurements at a wide temperature range (15–300 K). Possible recombination mechanisms are analyzed and compared in order to assess their influence on the free electron lifetime. It was found that nonradiative recombination at Zn-induced neutral acceptor centers is responsible for the short minority-carrier lifetime in this crystal down to a temperature of around 30 K. At lower temperatures three main processes determine the lifetime: radiative band-to-band recombination, radiative recombination in the deep acceptor level, and trapping at the shallow unintentional donor impurity centers.

DOI: 10.1103/PhysRevB.68.115210 PACS number(s): 78.55.−m, 78.60.−b, 78.20.−e, 71.55.−i

I. INTRODUCTION

The lifetime of excess carriers in semiconductors has been and continues to be of great interest both from technological and fundamental points of view.[1–4] From a fundamental point of view, it provides information on carrier scattering, capturing, and recombination mechanisms.[5–7] The technological importance is motivated by the performance of solid-state devices such as lasers, light-emitting diodes, and solar cells.[8] In the last decades there has been considerable interest in InP both as a prototypical III-V compound suitable for basic studies and as a potential candidate for a variety of electronic and optoelectronic devices. InP plays a crucial role in the high performance of $Ga_{1-x}In_xAs_{1-y}P_y$ (Ref. 9) and $Ga_{1-x}In_xAs$ (Ref. 10) avalanche photodiodes, lasers, and light emitting diodes. It also has important applications in integrated electron optics and in a variety of microwave and high-speed digital circuits[11] due to its high saturation drift velocity and high mobility. Recently, InP solar cells have been recognized as having great potential for space applications because of their extraordinary radiation resistance[12] and high efficiency.[13]

In spite of the numerous applications of InP, little has been done regarding study of its bulk lifetime and carrier recombination mechanisms. In a recent review article[14] it has been shown that the lifetimes measured in *n*-type crystals are in the range of 1–3000 ns (at 300 K), depending on crystal quality and growth methods. In the past we have shown[16] that at 300 K in Si-doped *n*-InP ($n_0=4.8\times10^{16}$ cm^{-3}) the dominant bulk recombination mechanism is radiative. On the other hand, the lifetime of electrons in *p*-InP was found to be much shorter and the dominance of nonradiative recombination was suggested.[15–17] Based on the data published during the last decade we can conclude that the lifetimes in *n*-type samples are typically two orders of magnitude larger than that of *p*-type InP. A similar trend was found for CdTe,[18,19] although it is based on a smaller number of measurements.

It is well known that the bulk minority-carrier recombination lifetime in semiconductors varies by many orders of magnitude, depending upon doping type, impurity concentration, and growth technique.[21] Even though the lifetime data is so disperse, one apparent trend is found in several direct bandgap semiconductors in general and in InP in particular. The trend is that *the bulk nonradiative recombination lifetime measured in n-type semiconductors is usually equal or larger than that measured in p-type semiconductors doped to the same level*. We have never found a case in which the nonradiative recombination lifetime in *n*-type semiconductors is shorter than that measured in *p*-type semiconductors with the same doping concentration. A similar trend was also found by measurements conducted by many other groups.[12,14,17]

We have carried out an extensive and systematic study of the carrier recombination in both *n*- and *p*-type InP using temperature-dependent time-resolved photoluminescence (TRPL) method. It is found that for *p*-InP the lifetime is very short due to a dominant deep neutral acceptor levels. On the other hand, in *n*-InP the recombination at high temperatures (>100 K) is governed by radiative band-to-band transitions.[20] In this manuscript we report on the study of *p*-InP. The experimental methods and results are described in Secs. II and III, respectively, and a detailed theoretical analysis is presented and discussed in Sec. IV.

II. EXPERIMENTAL

The samples were LEC grown (100) wafers of Zn-doped InP with two doping levels: $N_A=4\times10^{16}$ cm^{-3} (Crystacomm Inc.) and $N_A=1.5\times10^{16}$ cm^{-3} (Nippon Minning, Inc.). All the presented experimental data corresponds to the ''Crystacomm, Inc.'' sample; almost identical results were obtained for the other sample (Nippon Minning, Inc.). The samples were etched by aqua-regia and rinsed by deionized water before the measurements.

The TRPL setup, described in detail in Refs. 20 and 22, is based on a cw diode-pumped Nd:YAG laser (Millennia, Spectra Physics, Inc.) pumping a Ti-sapphire laser (Tsunami,

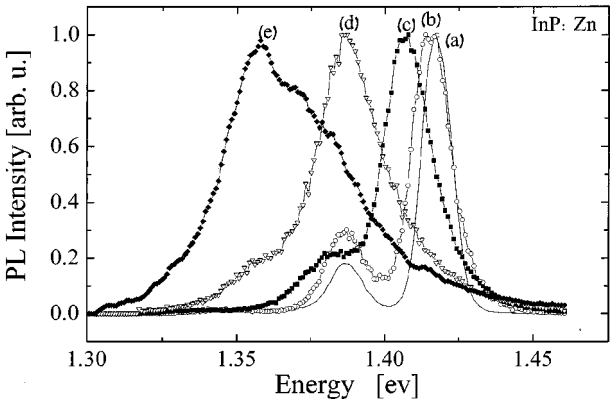

FIG. 1. Typical photoluminescence spectra of p-InP measured at five different temperatures of a: 15, b: 65, c: 120, d: 200, and e: 270 K.

Spectra Physics, Inc.), which provides high repetition rate (80 MHz) of short pulses with full width at half maximum of about 1.1 ps. The laser repetition rate is reduced using a pulse picker (model 3980, Spectra Physics, Inc.) to a rate of 4 MHz or 800 kHz. The laser beam power (typically at 730 nm) and spot size are adjusted to create an initial electron-hole concentration from 10^{14} cm^{-3} up to 5×10^{18} cm^{-3} in order to prevent crystal heating and surface damage. The photoluminescence (PL) emitted from InP is collected by a combination of a subtractive double monochromator, a cooled multichannel plate photomultiplier (Hamamatsu R3809) and a time-correlated single-photon-counting (TC-SPC) system. The overall instrument response (full width at half maximum) is about 30 ps.

III. RESULTS

A. Energy resolved PL spectra

Figure 1 shows a typical temperature dependence of the steady state photoluminescence (PL) spectra of a Zn-doped InP sample. The figure presents the steady state PL spectra of one of the Crystacomm samples ($N_A=4\times10^{16}$ cm^{-3}), where *a*, *b*, *c*, *d*, and *e* correspond to temperatures of 15, 65, 120, 200, and 270 K, respectively. Similar spectra were obtained for the p-InP samples of Nippon, Inc.

In order to correctly analyze the PL decay of the measured PL peaks observed in the energy-resolved spectra, the measurements were carried out in the following manner. All the PL spectra were measured under ''quasi-steady-state'' conditions, i.e., excitation with the pulsed laser (using the same carrier injection levels as in the time-resolved measurements presented below) and recording the time-integrated luminescence intensity. This is because TRPL measurements have to be conducted under relatively high injection conditions [$\Delta n(t=0)\geqslant1\times10^{14}$ cm^{-3}] in order to have a reasonable PL signal at short times ($\sim$30 ps) following excitation. Under such injection levels, the PL peaks are wide, typically 10–20 meV at full width at half maximum (FWHM), at $T=15$ K. In such a case many adjacent PL transitions of different nature, mainly these involving shallow donor and excitonic transitions, overlap. Another way to overcome this difficulty is to measure the energy-resolved PL spectra at very long delay times (microseconds) after the laser pulse; at such time the excess carrier concentration is very low, and the fast radiative recombination processes are not observed. Using such approach, Gilinsky *et al.* have been able to observe very shallow-acceptor-related PL transitions in high purity GaAs.[23]

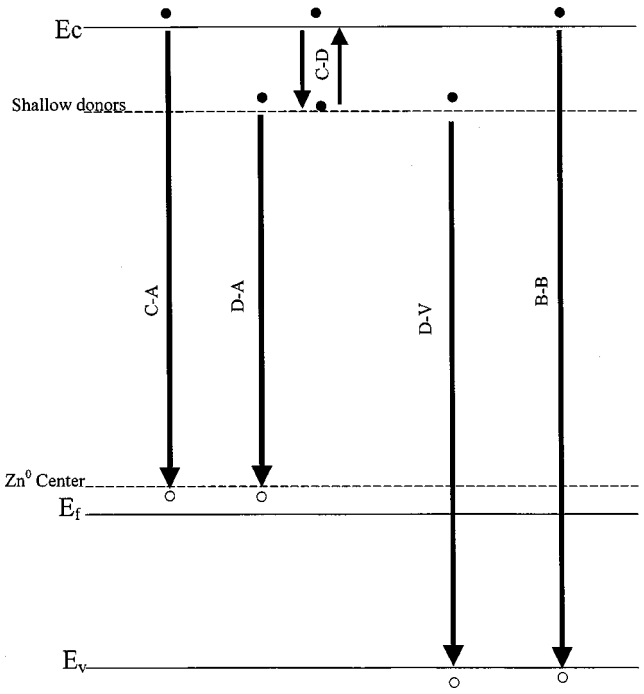

FIG. 2. Schematic energy bands diagram showing the main transitions for excess electrons in p-InP.

The PL spectra in Fig. 1 show two PL peaks at low temperatures and a single relatively broad peak, located around the bandgap energy above a temperature of $\sim$200 K. Below this temperature the second peak appears as a shoulder of the *B-B* peak at the energy of 36 meV below the first peak. The intensity of this peak increases with decreasing temperature as observed in the figure. This peak has been previously attributed by many authors to conduction band-to-acceptor (*C-A*) or donor-to-acceptor (*D-A*) transitions.[24–32] All the measured PL spectra indicate that no distinct donor impurity band exists in any of the *p*-type samples. Such a band should appear at 7–10 meV below the *B-B* peak[29] at very low temperatures due to donor-to-valence band (*D-V*) transition. This peak is not observed at any of our spectra due to two reasons: first, the very low concentration of unintentional shallow donor states in p-InP, and second, the FWHM of the *B-B* peak at 15 K is around 12 meV, thus it is merged with this peak. Therefore each of the two main PL peaks appearing in our spectra is a superposition of several transitions.

The main transitions in p-InP (at temperatures$>$15 K) are summarized in Fig. 2. The two peaks observed in our PL spectra, and which are studied by TRPL, are the *B-B* transition (overlaps with the *D-V* transition, here after called the band edge peak) and the *C-A* transition, which overlaps with the *D-A* transition, here after called the acceptor PL peak. The energy separation between the band edge and acceptor

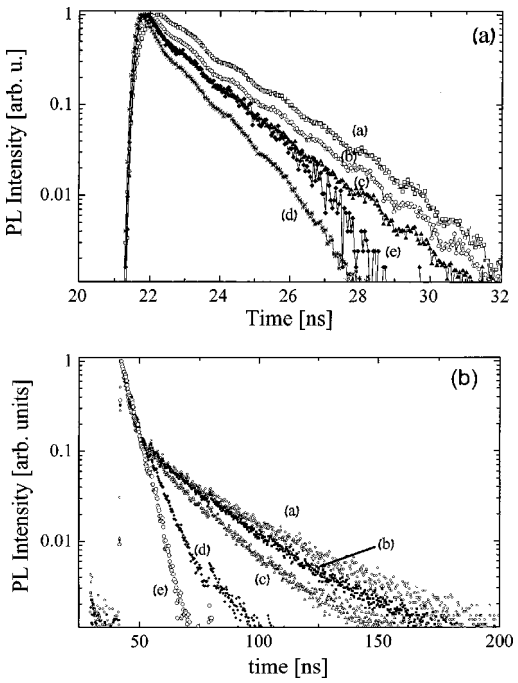

FIG. 3. (a) Photoluminescence decay curves of the band-to-band PL peak measured under low injection levels at temperatures of a: 15, b: 30, c: 45, d: 120, and e: 300 K; (b) Photoluminescence decay curves of the acceptor (subbandgap) PL peak measured at five different temperatures of a: 14, b: 18, c: 24, d: 34, and e: 39 K; the TRPL spectra did not change at temperatures higher then 39 K.

peaks is constant with temperature at a value of around 36 meV; this is consistent with Zn-induced acceptor states in InP.[26] In both cases the temperature dependence of the PL energy is consistent with the bandgap-energy temperature dependence of InP.[29] Though not visible on the linear scale of Fig. 1, a third peak located ~40 meV below the *C-A* peak, can be observed when using a logarithmic scale for the PL intensity. This peak is attributed to the LO phonon replica of the *C-A* transition in agreement with the LO phonon energy for InP of 42.8 meV.[33]

B. Time-resolved photoluminescence

The TRPL spectra, measured under low excitation conditions ($\Delta n = \Delta p \leqslant 10^{15}$ cm^{-3}), are presented in Fig. 3. Figure 3(a) shows the TRPL spectra of the band edge peak measured at temperatures of a: 15, b: 30, c: 45, d: 120, and e: 300 K; Fig. 3(b) shows the TRPL spectra of the subbandgap acceptor PL peak measured at temperatures of a: 14, b: 18, c: 24, d: 34, and e: 39 K. The TRPL spectra of the second peak did not change at temperatures higher than 39 K.

The effective electron lifetime value τ was extracted from these TRPL data. The method, described in the past,[16] is based on comparing calculated and experimental PL decay profiles. The normalized, time-dependent PL intensity $I(t)$ is calculated for a semi-infinite crystal as

$$I(t) = \int_0^\infty (n_0 + \Delta n)(p_0 + \Delta p)\exp(-\alpha_L x)dx, \qquad (1)$$

where α_L is the absorption coefficient for the gap-luminescence wavelength, and p_0 and n_0 are the equilibrium concentrations of holes and electrons, respectively. Assuming that the excess electron concentration Δn is balanced by the excess hole concentration Δp (local electroneutrality), that is

$$\Delta p(x,t) = \Delta n(x,t) \equiv \Delta C(x,t), \qquad (2)$$

the value of $\Delta C(x,t)$ can then be calculated using the ambipolar diffusion equation

$$\frac{\partial \Delta C(x,t)}{\partial t} = D^* \frac{\partial^2 \Delta C(x,t)}{\partial x^2} - \frac{\Delta C(x,t)}{\tau} + g(x,t), \qquad (3)$$

where the generation function is given by

$$g(x,t) = g_0(t)\alpha \exp(-\alpha x). \qquad (4)$$

D^* is the ambipolar diffusion constant, $g_0(t)$ is the generation rate defined by the temporal shape of the exciting laser pulse, and α is the absorption coefficient at the laser wavelength.

The boundary conditions for Eq. (3) are

$$\left.\frac{\partial \Delta C}{\partial x}\right|_{(x=0,t)} = \frac{S}{D^*}\Delta C(x=0,t),$$

$$\Delta C(x \to \infty, t) = 0, \quad \Delta C(x, t=0) = 0, \qquad (5)$$

where S is the effective surface recombination velocity. We have used the well known analytical solution for Eq. (3) (Refs. 16 and 34) derived by Vaitkus in order to extract the effective bulk lifetime from the TRPL data.

There are several approximations in using the Vaitkus analytical solution for the experimental data. First, the ambipolar equation is valid only under high injection (flatband) conditions. Since in this study we are interested only in low injection bulk (and not surface) recombination processes, all the measurements are conducted in the presence of surface electric field. The main effect of such a field is to drift the minority carriers (electrons) towards the surface and increase the surface recombination rate. This effect has been calculated by us in the past, and was found to affect only the first part (1–2 ns) of the PL decay curve.[35] Moreover, since we are interested here in fitting the bulk lifetime, the surface effect is not important; in any case S, the surface recombination velocity should be regarded as the effective velocity at the edge of the space charge region. Second, as will be shown below (Sec. IV E), the PL decay of the second peak is also affected by the trapping in the shallow donor states at low temperatures. Thus in order to accurately model the PL decay of this peak, this trapping process must be included in the model using the appropriate rate equation (describing the carrier trapping and emission from the shallow level[19]) coupled to the electron continuity equation. Thus we consider the fit to the experimental data [based on the analytical solution of Eq. (3)] as a good approximation that allows us to determine the different recombination processes, and to estimate the recombination parameters. A more accurate model including the shallow trapping level kinetics is in preparation.

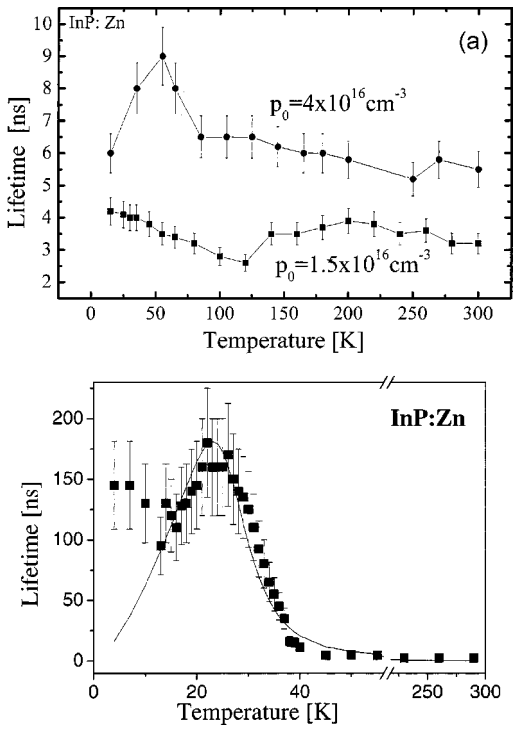

FIG. 4. (a) The effective bulk lifetime (τ) as a function of temperature extracted from fitting the PL decay of the band edge PL peak, Fig. 3(a). The error bars account for the accuracy ($\pm 10\%$) of the fitting process. (b) The effective lifetime (τ) as a function of temperature extracted from fitting the PL decay of the acceptor PL peak, Fig. 3(b). The solid line is a fit to the experimental data based on Eq. (43).

The temperature dependencies of the bulk effective lifetime values, extracted from fitting the PL decays of the band edge (for two of the measured p-InP samples) are shown in Fig. 4(a); the small difference in lifetime (4 versus 6 ns at high temperatures) is attributed to sample growth quality and not to any significant physical reason. Figure 4(b) shows the effective lifetime extracted in a similar manner for the acceptor PL peak. The following parameters were used in the fitting procedure: absorption coefficient at the exciting laser wavelength $\alpha = 2\times 10^4$ cm^{-1}, absorption coefficient at the PL wavelength $\alpha_L = 3\times 10^3$ cm^{-1}, the ambipolar diffusion coefficient D^* (300 K) = 5 cm^2/s, and an effective surface recombination velocity $S = 1\times 10^4$ cm/s. The diffusion coefficient temperature dependence $D(T)$ was calculated using the well known Einstein relation and the temperature dependence of the mobility in InP.[14,43] A visual fit to the data was performed by changing only the effective bulk lifetime, τ, and keeping all the other parameters constant.

The error bars represent the accuracy ($\pm 10\%$) of the fitting process; in other words, such a change in τ would result in a similar quality visual fit to the data. It is observed that the effective PL lifetime corresponding to the band edge [Fig. 4(a)] is almost unchanged with temperature in the range 15–300 K, while that of the second peak changes drastically in the 14–40 K temperature range and then stays more or less constant close to the value of the band edge PL peak. In the next section these trends are analyzed in detail, and it is shown that the deep Zn^0 neutral acceptor centers are governing the recombination processes in p-InP and are responsible for the short minority-carrier lifetime in this semiconductor.

IV. ANALYSIS

A. General

In the analysis of the PL data we will distinguish between the band edge and the acceptor PL peaks and will take into account their complex character. The band edge peak is a superposition of at least two radiative transitions: the band-to-band transition, and a transition from the unintentional shallow donor states to the valence band. At low temperatures the luminescence caused by recombination of free and bound excitons is also present.[26] Only at relatively high temperatures when the contribution of the exciton recombination is suppressed, and the shallow donor states are all ionized, the decay rate of the band edge peak represents directly the recombination kinetics of the conduction band electrons. The second luminescence peak is a superposition of two radiative processes: radiative transitions of electrons from the conduction band to the deep acceptor level and tunneling recombination of electron-hole pairs localized at the donor and acceptor states, respectively. Below we analyze in detail six main recombination processes that affect the minority carrier lifetime. By comparing the calculations to the decay rate of the acceptor PL peak we show that the dominant recombination process is the nonradiative recombination at the deep acceptor levels (*C-A* transition). This process is responsible for the very short electron lifetime at temperatures higher then 40 K found in p-InP.

B. Radiative band-to-band recombination

The radiative band-to-band electron lifetime in p-type semiconductors under low carrier injection levels is given by[36]

$$\tau_{CV} = \frac{1}{B[\Delta p + p_0(T)]}, \tag{6}$$

where B is the radiative rate constant, given by[37]

$$B = \frac{(2\pi)^{3/2}\hbar e_0^2 n_r}{c m_0^{5/2}(kT)^{3/2}}\left(\frac{m_0}{m_e+m_h}\right)^{3/2}\left(1+\frac{m_0}{m_e}+\frac{m_0}{m_h}\right)E_g^2, \tag{7}$$

where m_e is the electron effective mass in the conduction band, m_h is the hole effective mass in the valence band, m_0 is a free electron mass, n_r is a refractive index, and c is the velocity of light. The temperature dependence of the radiative recombination rate constant may be written as $B = B_0(300/T)^{3/2}$, where $B_0 = 2\times 10^{-11}$ cm^3 s^{-1} for InP crystals.[16] Even when $p = 4\times 10^{16}$ cm^{-3} (complete acceptor ionization), the corresponding radiative lifetime $\tau_r \geqslant 500$ ns. Comparing this value with the measured effective bulk lifetime shows that the radiative band-to-band recombination cannot be the dominant mechanism in p-InP at least at high temperatures.

C. Nonradiative Auger recombination

Nonradiative recombination can be carried out through an Auger process, where the recombination energy is transferred to a third carrier, free or bound, and hence it is significant only at very high carrier concentrations.[36,38] The electron lifetime for this process is given by[38]

$$\tau_{\text{Auger}}=\frac{1}{C_p p p_A}, \tag{8}$$

where p_A is the concentration of bound holes in the corresponding gap level, and C_p is the Auger recombination coefficient, that at room temperature in InP is equal to 6.1×10^{-29} cm^6 s^{-1}.[38] For $p=p_A=4\times10^{16}$ cm^{-3} the Auger lifetime $\tau_{\text{Auger}}=4.1\times10^{-5}$ s; this value is at least three orders of magnitude larger than that measured in this study. In summary, neither nonradiative Auger processes, nor radiative band-to-band recombination processes can account for the very short electron lifetime (few ns) measured in p-InP.

D. Donor-acceptor tunneling recombination

The electron located at a donor atom D is capable of tunneling to an acceptor A and recombining with the hole, localized in this acceptor. The probability that an electron tunnels a distance r between a donor and an acceptor state is[39]

$$W(r)=W_0\exp(-r/r_0) \tag{9}$$

where W_0 is the coefficient with the dimensions of the frequency and r_0 is a parameter representing the decay of the wave functions of the donor and acceptor. Usually the donor radius r_d is much larger than the acceptor radius. In such a case

$$r_0=\frac{1}{2}r_d. \tag{10}$$

The probability of an electron present in a donor at time t is[39]

$$Q(t)=e^{4\pi p_A\int_0^\infty[e^{-W(r)t}-1]r^2dr}, \tag{11}$$

where p_A is the hole concentration in the acceptors. Differentiating $Q(t)$ with respect to time, we obtain

$$\frac{dQ(t)}{dt}=-W_{\text{tun}}(t)Q(t), \tag{12}$$

where

$$W_{\text{tun}}(t)=4\pi p_A\int_0^\infty W(r)e^{-W(r)t}r^2dr \tag{13}$$

is the tunneling rate at time t. From Eqs. (9) and (13) we obtain

$$W_{\text{tun}}(t)=8\pi p_A W_0 r_0^3\sum_{n=0}^{\infty}\frac{[-W_0t]^n}{(n+1)!(n+1)^2}. \tag{14}$$

The highest tunneling probability will be at $t=0$, hence using Eq. (14) we obtain

$$W_{\text{tun}}(t=0)=B_{\text{tun}}p_A, \tag{15}$$

where

$$B_{\text{tun}}=8\pi W_0 r_0^3 \tag{16}$$

is the D-A tunneling recombination rate constant. In InP: $W_0=6.5\times10^7$ s^{-1}, $r_0=5\times10^{-7}$ cm[25], so the rate constant $B_{\text{tun}}=2\times10^{-10}$ cm^3/s.

E. Radiative recombination at the deep acceptor levels

Radiative optical transitions, involving impurities, were analyzed by Dumke.[40] For free electrons, recombining with p_A bound holes, the radiative transition lifetime is given by

$$\frac{1}{\tau^r_{C\text{-}A}}=B^0_{C\text{-}A}p_A\Gamma_C(\alpha), \tag{17}$$

where

$$B^0_{C\text{-}A}=64\sqrt{2}\pi n_r\frac{e^2\hbar^2\omega|P_{V\text{-}C}|^2}{c^3m_0^2(m_hE_A)^{3/2}} \tag{18}$$

is the corresponding radiative rate constant at $T=0$ K. The function $\Gamma_C(\alpha)$ accounts for the decrease in the radiative transition probability caused by the thermal filling of the states in the conduction band $\alpha=m_hE_A/m_ekT$, $\hbar\omega$ is the photon emission energy, E_A is the acceptor binding energy, and P_{VC} is the interband matrix element of the momentum operator given in Ref. 42 as $|P_{VC}|^2\approx m_0E_g$. Using Eq. (7), and the values of $m_e=0.0765m_0$, $m_h=0.635m_0$,[41] and $E_A=36$ meV (from the PL spectra), we have calculated the ratio between the rate constants of the band-to-band, and the C-A radiative transitions

$$B_{C\text{-}A}(T)=0.762B_0\Gamma_C(T). \tag{19}$$

We can now compare the contribution of the D-A tunneling recombination, and the C-A transition to the intensity of the second luminescence peak. If Δn is the electron concentration in the conduction band, the C-A luminescence intensity is equal to

$$I_{C\text{-}A}=\frac{\Delta n}{\tau^r_{C\text{-}A}} \tag{20}$$

The luminescence intensity due to the D-A tunneling recombination is proportional to the concentration of the occupied donors N_d

$$I_{\text{tun}}=N_dW_{\text{tun}}(t=0)=B_{\text{tun}}N_dp_A. \tag{21}$$

Thus the ratio of the luminescence intensities of these two transitions is given by

$$\frac{I_{C\text{-}A}}{I_{\text{tun}}} = \frac{0.762 B_0 \Gamma_c(T) \Delta n}{B_{\text{tun}} N_d}. \tag{22}$$

Our calculations show that in InP the factor $\Gamma(T)$ changes from 1 to 0.7 when the temperature changes from 4 to 300 K. Thus the ratio of the luminescence intensities [Eq. (22)] depends mainly on the ratio between the excess carrier concentration Δn and the occupied donor concentration N_d. In crystals with high donor concentration $N_d \gg \Delta n$ (this happens under low injection levels and at low temperatures), the second peak is governed by tunneling recombination; such a case was reported in Refs. 24, 26, and 27, where N_d was $\geqslant 10^{16}$ cm^{-3}. However (as will be shown below), the density of shallow traps in our *p*-type samples, resulting from unintentional doping, is only around 10^{12} cm^{-3}. Thus at the typical injection levels used in our experiments, $\Delta n \sim 10^{15}$ cm^{-3}, the *C-A* radiative recombination rate is about a factor of 50–70 larger than the *D-A* tunneling recombination rate. In summary, in *p*-InP crystals the second peak luminescence intensity and its decay rate are effectively determined by the kinetics of the conduction band electrons (the *C-A* transition). Therefore below we focus our analysis on the TRPL of the second luminescence peak, which gives direct information about the minority carrier lifetime.

F. Nonradiative recombination at the deep acceptor level

In Zn-doped InP crystals the dominant nonradiative recombination centers are the neutral Zn centers, formed as a result of the doping process. The nonradiative recombination of free carriers in deep centers was first discussed in detail by Henry and Lang,[42] and then by many others.[43,44] A good review on this subject can be found in Ref. 36. In general the temperature dependence of the excess carrier recombination cross section $\sigma_R(T)$ is very complicated. However, at sufficiently high temperatures the capture results from lattice thermal vibrations causing the crossing of the conduction band electron and the deep trap states. In such a case $\sigma_R(T)$ may be described by the nonradiative capture with lattice-relaxation multiphonon emission in the following form:[38]

$$\sigma_R = \sigma_0 \exp(-E_{\text{ac}}/kT), \tag{23}$$

where E_{ac} is an activation energy equal to the vibration energy of free carrier state at the intersection with the bound state. Hence the resulting electron lifetime due to nonradiative recombination in the deep level is given by

$$\frac{1}{\tau_{C\text{-}A}^{nr}} = p_A \sigma_R \upsilon_e, \tag{24}$$

where υ_e is the mean electron thermal velocity in the conduction band. According to Eqs. (23) and (24) the electron lifetime $\tau_{C\text{-}A}^{nr}$ increases with decreasing temperature due to the decrease of the recombination cross section.

At low temperatures such an activation process is suppressed and the necessary states crossing may be achieved by lattice vibration tunneling at energies significantly less than E_{ac}. The theory of multiphonon nonradiative capture was reported by many authors (for example, Ref. 38, 44, 45, and references within); we base our analysis below on the theory suggested by Abakumov *et al.*[45]

It is generally accepted that in several recombination mechanisms only a single vibration mode is dominant in the multiphonon capture; thus the electron practically interacts only with this oscillation (the so-called activating mode); in such a case the capture cross section has the form

$$\sigma = A \exp(-\Phi), \tag{25}$$

where Φ is a function that depends on temperature, on the electron binding energy, on the phonon energy, and on the dimensionless coupling constant $\beta = \Delta E / E_{\text{opt}}$. This constant is the ratio between the polaron energy shift ΔE and the energy required for optical excitation from the impurity state into the conduction band E_{opt}.

Below we show that the constant β is very small ($\sim 10^{-3}$) for shallow acceptor centers in InP, thus we neglect the temperature dependence of Φ on β, and it takes the form

$$\Phi = \frac{E_t}{\hbar\omega} \ln\left[1 - \exp\left(-\frac{\hbar\omega}{kT}\right)\right], \tag{26}$$

where E_t it the impurity thermal ionization energy and $\hbar\omega$ is the phonon energy with which the captured electron actively interacts. From Eqs. (24) and (25) we obtain

$$\sigma = \frac{A}{(1 - e^{-\hbar\omega/kT})^{E_t/\hbar\omega}}. \tag{27}$$

In the general case the constant A is expressed as[45]

$$A = C\left(\frac{\hbar\omega}{kT}\right)^2 \sinh\left(\frac{\hbar\omega}{2kT}\right) \frac{(1-z_0)^{1/2}[1-(1-\beta)z_0]^{1/2}}{\{z_0^{1/2} \ln[(1+z_0^{1/2})/(1-z_0^{1/2})]\}^{3/2}}, \tag{28}$$

where the constant C is temperature independent and the parameter z_0 is

$$z_0 = 1 - \frac{\beta}{(1-\beta)} \frac{1}{(e^{\hbar\omega/kT} - 1)}$$

which for $\beta \ll 1$ becomes

$$z_0 = 1 - \frac{\beta}{(e^{\hbar\omega/kT} - 1)}.$$

Inserting z_0 in Eq. (28) and then the preexponential factor A in Eq. (27) we obtain

$$\sigma(T) = \sigma_0 \left(\frac{\hbar\omega}{kT}\right)^2 \frac{e^{-\hbar\omega/2kT}}{\left\{\ln\left[\frac{4}{\beta}(e^{\hbar\omega/kT} - 1)\right]\right\}^{3/2} (1 - e^{-\hbar\omega/kT})^{E_t/\hbar\omega}} \tag{29}$$

where σ_0 is a temperature independent constant. Equation (29) differs from that derived by Abakumov *et al.* in Ref. 45 by the factor $e^{-\hbar\omega/2kT}$ that plays an important role at low temperatures. For $T \ll \hbar\omega/2k$ the energy of zero oscillation of the active phonon mode, $E_{\text{eff}} = \hbar\omega/2$ is the effective activation energy.

In order to determine the coupling constant β for the Zn center in InP, the polaron shift ΔE has to be calculated. In polar crystals the electron interaction with the longitudinal optical phonons is the main contribution to ΔE, and its value may be deduced from the intensity ratio of the first LO-phonon replica to the phononless luminescence peak. In the case of weak coupling this ratio equals $S = S_0 \mathrm{cotanh}(\hbar\omega/2kT)$ where S_0 is the Huang-Rhys factor[46] and determines the average number of the emitted phonons as a result of optical transition. Our experimental data show that at low temperatures, defined by $T \ll \hbar\omega/2k$ ($\sim$260 K), the intensity ratio equals to $S \approx S_0 = \Delta E/\hbar\omega_{\mathrm{LO}} = 0.05$. Almost the same ratio of 0.055 was obtained by Röder *et al.*[27] in InP for the phononless peak at 1.37 eV and its LO-phonon replica; the polaron energy shift is thus equal to $\Delta E = S\hbar\omega_{\mathrm{LO}} = 2.15$ meV. The radiative electron capture from the conduction band to the acceptor Zn level results in a photon emission at an energy of $E_{\mathrm{lum}} = 1.37$ eV. Thus the corresponding energy of the optical ionization exceeds the luminescence energy by the Stokes shift equal to $2\Delta E$: $E_{\mathrm{opt}} = E_{\mathrm{lum}} + 2\Delta E$.

In our case $E_{\mathrm{opt}} = 1.374$ eV and hence the binding constant $\beta = \Delta E/E_{\mathrm{opt}} = 1.56 \times 10^{-3}$. Equation (29) shows that the temperature dependence of the multiphonon capture cross-section strongly depends on the ratio of E_t and $\hbar\omega$. The thermal ionization energy of the Zn center is $E_t = E_{\mathrm{lum}} + \Delta E = 1.372$ eV; the phonon energy $\hbar\omega = 43.3$ meV and $\sigma_0 = 1.35 \times 10^{-13}$ cm^2 were determined from fitting the PL data as shown in Sec. V below. This value of $\hbar\omega$ is in an excellent agreement with the energy of the LO phonons in InP; for example infrared reflectivity and Raman measurements gave values of 43 and 42.8 meV respectively.[47,48]

This result is also in agreement with the radius of the localized state $r_a = \hbar/\sqrt{2m^* E_B} = 12.6$ Å which significantly exceeds the interatomic distance in the InP lattice (2.54 Å); thus the electron wave function hardly overlap with the local impurity oscillation. Thus the localized electron actively interacts only with the LO phonons, which are emitted in the process of the nonradiative electron capture. If the function $\sigma(T)$ is approximated by the simple exponential dependence of Eq. (23), the activation energy is 21 meV, approaching the zero oscillation energy $\hbar\omega_{\mathrm{LO}}/2 = 21.65$ meV. Such temperature dependence is obtained from Eq. (29) at high temperatures.

G. The effect of the shallow trapping levels

As the temperature decreases the shallow traps capture the photogenerated electrons. We will show below that at temperatures between 15–30 K these traps change significantly the conduction band electron lifetime. At low temperatures the electron trapping probability in the shallow ionized donor centers depends on their concentration N_t, and on the effective trapping cross section σ_t through

$$\frac{1}{\tau_t} = N_t \sigma_t \upsilon_e . \tag{30}$$

According to Ref. 43 the value of σ_t is a product of the capture and the emission probability from the trap

$$\sigma_t = \sigma_c \frac{W_{\mathrm{rec}}}{e_n + W_{\mathrm{rec}}}, \tag{31}$$

where σ_c is the electron capture cross-section in a charged shallow center, e_n is the thermal ionization rate from the trap, given by[36]

$$e_n = \frac{1}{g}\sigma_c \upsilon_e N_c \exp\left(-\frac{E_d}{kT}\right), \tag{32}$$

where N_c is the effective density of states in the conduction band, and g and E_d are the degeneracy factor and the ionization energy of the donor level, respectively. W_{rec} is the total recombination rate of an electron captured in the trap, explained in detail below.

The cross section σ_c was first calculated by Lax,[49] and the theory was further developed by Abakumov *et al.*[38] According to this theory (''the nonradiative cascade capture''), a conduction band electron can be trapped by the high-excited states of the trap, and then can be reemitted into the conduction band or can make cascade transitions into a lower excited state by emission of one acoustic phonon. It was shown[38] that the cross section of a free carrier capture in a singly charged center is equal to

$$\sigma_c = \frac{4\pi}{3 l_0}\left(\frac{e^2}{\varepsilon kT}\right)^3, \tag{33}$$

$$l_0 = l\frac{kT}{2m_e s^2}, \tag{34}$$

where ε is the semiconductor dielectric constant, $l = \upsilon_e \tau_e$ is the electron mean free path due to collisions with acoustic phonons, τ_e is the corresponding energy relaxation time, and s is the speed of sound. At $T = 77$ K in InP the electron mobility $\mu_e = 5 \times 10^4$ cm^2/s,[14] and as a result at this temperature $\tau_e = 2.2 \times 10^{-12}$ s, and from Eq. (34) using $s = 5.1 \times 10^5$ cm/s then $l_0 = 1.25 \times 10^{-2}$ cm. Using these parameters the cross section for electron capture in the shallow trap will be

$$\sigma_c = 2.9 \times 10^{-17}(300/T)^3 \ \ \mathrm{cm}^2. \tag{35}$$

The net recombination rate of electrons in the shallow level is determined by the cross section σ_t [Eq. (31)], which takes into account three processes by which the electrons leave the shallow levels. These include tunneling to the acceptors, and recombination (either radiatively or nonradiatively) with free holes in the conduction band:

$$W_{\mathrm{rec}} = W_{\mathrm{tun}} + W^r_{D\text{-}V} + W^{\mathrm{nr}}_{D\text{-}V} \tag{36}$$

Here $W^r_{D\text{-}V}$ and $W^{\mathrm{nr}}_{D\text{-}V}$ are the recombination rates of the radiative and nonradiative D-V transitions, respectively. The radiative D-V transition is analyzed using the theory presented by Dumke.[40] The donor to valence band radiative recombination rate can be written as

$$W^r_{D\text{-}V} = B_{D\text{-}V}[\Delta p + p_0(T)], \tag{37}$$

where $p_0(T) \equiv N_A - p_A(T)$ is the equilibrium hole concentration in the valence band. The recombination rate constant $B_{D\text{-}V}$ is given by

$$B_{D\text{-}V} = \frac{64\sqrt{2}\pi n_r \hbar E_g |P_{V\text{-}C}|^2 e_0^2 \Gamma_V(T)}{c^3 m_0^2 (m_e E_D)^{3/2}}, \tag{38}$$

where E_D is the donor binding energy and $\Gamma_V(T)$ accounts for the decrease in the radiative transition probability caused by the thermal filling of the states in the valence band. If the emitted photon energy is assumed to be equal to the band gap, we obtain

$$B_{V\text{-}D} = \frac{64\sqrt{2}\pi n_r \hbar E_g^2 e_0^2 \Gamma_V(T)}{c^3 m_0 (m_e E_D)^{3/2}}. \tag{39}$$

Using Eq. (7) and $E_D = 7$ meV,[14,40] the ratio between the rate constants of the radiative D-V transition and the band-to-band radiative transition B_0 is

$$B_{V\text{-}D} = 238 B_0 \Gamma_V(T). \tag{40}$$

Calculating $\Gamma_V(T)$ taking into account both the light and heavy holes it is found that it changes from 0.1 (15 K) to 2×10^{-3} (300 K).

For the analysis of the nonradiative D-V recombination process the model, proposed by Lax,[49] has been used. According to this model a free carrier (a hole in our case) polarizes the neutral donor center, inducing a dipole moment; the electric field of this dipole attracts the hole—this is the D-V nonradiative recombination process. Its recombination rate may be written as

$$W_{D\text{-}V}^{\mathrm{nr}} = \sigma_{D\text{-}V}(T) \upsilon_p [\Delta p + p_0(T)], \tag{41}$$

where $\sigma_{D\text{-}V}(T)$ is the cross section for hole capture in the electron occupied neutral donor center, and υ_p is the hole thermal velocity. Such a cross section was determined experimentally at low temperature for germanium.[50] It was shown that $\sigma_{D\text{-}V}(4.2\ \mathrm{K}) = 5 \times 10^{-16}\ \mathrm{cm}^2$ and it is proportional to T^{-2}; such temperature dependence agrees with the Lax model. Thus, the capture cross section $\sigma_{D\text{-}V}$ has to decrease to $10^{-19}\ \mathrm{cm}^2$ at 300 K. In our calculation we have used $\sigma_{D\text{-}V}$ in the form

$$\sigma_{D\text{-}V}(T) = A \left(\frac{300}{T} \right)^2 10^{-19}\ \ \mathrm{cm}^2, \tag{42}$$

where A is a fitting parameter

V. COMPARISON WITH THE EXPERIMENTAL RESULTS

According with the above analysis, the electron lifetime in p-type InP is determined by the following processes: radiative and nonradiative recombination in the neutral deep acceptor centers with lifetimes $\tau_{C\text{-}A}^r$ [Eqs. (17) and (19)] and $\tau_{C\text{-}A}^{\mathrm{nr}}$ [Eqs. (24) and (29)], respectively, electron trapping in the charged unintentional donor levels with a lifetime τ_t [Eqs. (30)–(42)], and a radiative band-to-band recombination characterized by τ_{CV} [Eq. (6)]. The effective bulk lifetime is then

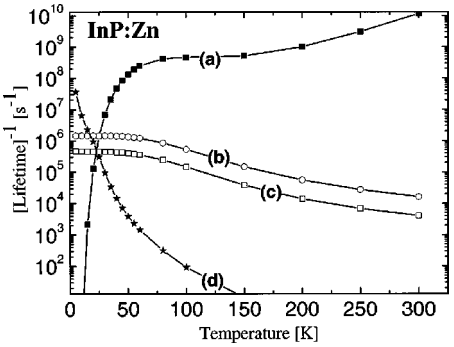

FIG. 5. The four main recombination processes in p-InP, calculated using Eq. (43) with the recombination parameters extracted from fitting the measured effective lifetime: (a): nonradiative A-C recombination, (b) radiative A-C recombination, (c) band-to-band radiative recombination, (d) trapping in the shallow donorlike centers.

$$\frac{1}{\tau} = \frac{1}{\tau_{C\text{-}A}^r} + \frac{1}{\tau_{C\text{-}A}^{\mathrm{nr}}} + \frac{1}{\tau_t} + \frac{1}{\tau_{C\text{-}V}}. \tag{43}$$

We can now use Eq. (43) to calculate the effective electron lifetime τ as a function of temperature. The calculated value can be fitted to the measured electron lifetime in order to extract the main recombination parameters.

The result of this fitting procedure is shown in Fig. 4(b). The figure shows the effective lifetime extracted from the TRPL data, represented by the error bars, together with a solid line, which is a fit of Eq. (44) to the experimental data. The fit enabled us to find five recombination parameters: the cross section and the phonon energy for the A-C nonradiative recombination process $\sigma_0 = 1.35 \times 10^{-13}\ \mathrm{cm}^2$ and $\hbar\omega = 43.3$ meV, respectively, the density of the donor-like trapping centers $N_t = 1.1 \times 10^{12} \pm 3 \times 10^{11}\ \mathrm{cm}^{-3}$, the cross section of the nonradiative donor-valence band recombination process $\sigma_{D\text{-}V} = (4.4 \pm 2.7) \times 10^{-19}\ \mathrm{cm}^2$ (300 K), and the band-to-band radiative rate constant $B_0(300\ \mathrm{K}) = (5.2 \pm 2.6) \times 10^{-11}\ \mathrm{cm}^2\ \mathrm{s}^{-1}$.

Using these constants the temperature dependence of the four main recombination processes can now be calculated. Figure 5 shows these four recombination rates (divided by Δn) as a function of temperature. The recombination rate in the deep acceptor level [curve (a)] decreases with decreasing temperature (effective lifetime increase) because the lattice thermal vibrations, driving this recombination process are suppressed at low temperatures. At low temperatures (below $\sim$30 K) the electron lifetime is determined by three main processes: radiative C-A [curve (b)] and C-V [band-to-band, curve (c)] transitions, and trapping at the shallow donorlike centers [curve (d)]. At temperatures above $\sim$30 K, the C-A nonradiative process [curve (a)] becomes the most efficient recombination channel and determines the electron lifetime.

Moreover, it is observed that the nonradiative C-A recombination lifetime reaches a value of a few nanoseconds at a temperature of around $\sim$80 K, and does not change significantly with increasing temperature. Due to the fact that the band edge and the acceptor PL peaks merge at a temperature

of around 100 K, we conclude that the *C-A* recombination process determines also the PL decay rate of the band edge PL peak.

VI. SUMMARY

We have presented a comprehensive study of minority carrier lifetime and recombination mechanisms in *p*-InP single crystals, based on steady state and time-resolved photoluminescence measurements at a wide temperature range (15–300 K). It was found that nonradiative recombination at Zn-induced neutral acceptor centers is responsible for the short minority carrier lifetime in this crystal down to a temperature of around 30 K. At lower temperatures the lifetime is determined by three main processes: radiative band-to-band recombination, radiative recombination in the deep acceptor level, and trapping at the shallow unintentional donor impurity centers. A fit of the measured effective bulk lifetime to a recombination model based on the main recombination processes enabled us to extract several important parameters: the cross section and the photon energy for the electron-neutral acceptor recombination rate, the density of the donor-like trapping centers, the cross section of the nonradiative donor-valence band recombination process, and the band-to-band radiative rate constant.

[1] L. Passari and E. Susi, J. Appl. Phys. **54**, 3935 (1983).
[2] R. J. Nelson and R. G. Sobers, Appl. Phys. Lett. **29**, 6103 (1978).
[3] R. K. Ahrenkiel, Solid-State Electron. **35**, 239 (1992).
[4] D. M. Kim, S. Lee, M. I. Nathan, A. Gopinath, F. Williamson, K. Beyzavi, and A. Ghiasi, Appl. Phys. Lett. **62**, 861 (1993).
[5] S. Raymond, S. Fafard, S. Charbonneau, R. Leon, D. Leonard, P. M. Petroff, and J. L. Merz, Phys. Rev. B **52**, 17 238 (1995).
[6] M. B. Johnson, T. C. McGill, and A. T. Hunter, J. Appl. Phys. **63**, 2077 (1988).
[7] S. M. Sze, *Physics of Semiconductor Devices* (Wiley, New York, 1971).
[8] F. S. Choa, J. Y. Fan, P.-L. Liu, J. Sipiro, G. Rao, G. M. Carter, and Y. J. Chen, Appl. Phys. Lett. **69**, 3668 (1996); R. K. Ahrenkiel, D. J. Dunlary, and T. Hanak, Sol. Cells **24**, 339 (1988).
[9] V. Diadiuk, S. H. Grove, C. E. Hurwitz, and G. W. Iseler, IEEE J. Quantum Electron. **QE-17**, 260 (1981).
[10] S. R. Forrest, G. F. Williams, O. K. Kim, and R. G. Smith, Electron. Lett. **17**, 917 (1981).
[11] L. Messick, D. A. Collins, and D. L. Lile, IEEE Trans. Electron Devices **7**, 680 (1986).
[12] M. Yamaguchi, C. Uemura, A. Yamamoto, and A. Shibukawa, Jpn. J. Appl. Phys. **23**, 302 (1984); I. Weinberg, C. K. Swartz, and R. E. Hart, (unpublished).
[13] R. K. Jain, I. Weinberg, and D. J. Flood, (unpublished); R. K. Jain and D. J. Flood, IEEE Trans. Electron Devices **41**, 2473 (1994).
[14] R. K. Ahrenkiel, *Properties of InP* (INSPEC, London, 1991), p. 77.
[15] J. A. Yater, P. Jenkins, G. A. Landis, and I. Weinberg (unpublished).
[16] Y. Rosenwaks, D. Huppert, and Y. Shapira, Phys. Rev. B **44**, 13 097 (1991).
[17] G. A. Landis, P. Jenkins, and I. Weinberg (unpublished).
[18] S. Bothra, S. Tyagi, S. K. Ghandhi, and J. M. Borrego, Solid State Electron. **34**, 47 (1991).
[19] R. Cohen, V. Lyahovitskaya, E. Poles, A. Liu, and Y. Rosenwaks, Appl. Phys. Lett. **73**, 1400 (1998).
[20] I. Tsimberova, Y. Rosenwaks, and M. Molotskii, J. Appl. Phys. **93**, 9797 (2003).
[21] R. K. Ahrenkiel, *Semiconductors and Semimetals* (Academic, New York, 1993), Vol. 39, Chap. 2.
[22] Y. Rosenwaks, Y. Shapira, and D. Huppert, Phys. Rev. B **45**, 9108 (1992).
[23] A. M. Gilinsky and K. S. Zhuravlev, Appl. Phys. Lett. **68**, 373 (1996).
[24] R. C. C. Leite, Phys. Rev. **157**, 672 (1967).
[25] U. Heim, O. Röder, and M. H. Pilkuhn, Solid State Commun. **7**, 1173 (1969).
[26] U. Heim, Solid State Commun. **7**, 445 (1969).
[27] O. Röder, U. Heim, and M. H. Pilkuhn, J. Phys. Chem. Solids **31**, 2625 (1970).
[28] J. B. Mullin, A. Royle, B. W. Straugham, P. J. Tufton, and E. W. Williams, J. Cryst. Growth **13/14**, 640 (1972).
[29] E. W. Williams, W. Elder, M. G. Astles, M. Webb, J. B. Mullin, B. Straugham, and P. J. Tufton, J. Electrochem. Soc. **120**, 1741 (1973).
[30] M. Yamaguchi, A. Yamamoto, S. Shinoyama, and H. Sugiura, J. Appl. Phys. **53**, 633 (1982).
[31] R. M. Sieg and S. A. Ringle, J. Appl. Phys. **80**, 448 (1996).
[32] M. Bugajski and W. Lewandowski, J. Appl. Phys. **57**, 521 (1985).
[33] V. Swaminathan and A. T. Macrander, *Materials aspects of GaAs and InP Based Structures* (Prentice-Hall, Englewood Cliffs, NJ, 1991).
[34] J. Vaitkus, Phys. Solid State **34**, 769 (1976).
[35] Y. Rosenwaks, B. R. Thacker, R. K. Ahrenkiel, A. J. Nozik, and I. Yavneh, Phys. Rev. B **50**, 1746 (1994).
[36] R. T. Landsberg, *Recombination in Semiconductors* (University Press, Cambridge, 1991), pp. 373–381;
[37] Y. P. Varshni, Phys. Solid State **19**, 459 (1967).
[38] V. N. Abakumov, V. I. Perel, and I. N. Yassievich, *Nonradiative Recombination in Semiconductors*, in *Modern Problems in Condenced Matter Sciences*, edited by V. M. Agranovich and A. A. Maradudin (North-Holland, Amsterdam, 1991), Vol. 33.
[39] D. G. Thomas, J. J. Hopfield, and W. M. Augustyniak, Phys. Rev. **140**, A202 (1965).
[40] W. P. Dumke, Phys. Rev. **132**, 1998 (1963).
[41] *Landolt-Börnstein, Numerical Data and Functional Relationships in Science and Technology*, edited by O. Madelung, M. Schulz, and H. Weiss, *Physics of Group IV Elements and III-V Compounds* (Springer, Berlin, 1982), Vol. 17a, pp. 281–297.
[42] C. H. Henry and D. V. Lang, Phys. Rev. B **15**, 989 (1977).
[43] R. M. Gibb, G. J. Rees, B. W. Thomas, B. L. H. Wilson, B. Hamilton, D. R. Wight, and N. F. Mott, Philos. Mag. **36**, 1021 (1977).

[44] A. M. Stoneham, Rep. Prog. Phys. **44**, 1251 (1981).
[45] V. N. Abakumov, I. A. Merkulov, V. I. Perel, and I. N. Yassievich, Zh. Eksp. Teor. Fiz. **89**, 1472, 1985 [Sov. Phys. JETP **62**, 853 (1985)].
[46] A. M. Stoneham, *Theory of Defects in Solids* (Clarendon Press, Oxford, 1975).
[47] R. Newman, Phys. Rev. **111**, 1515 (1958).
[48] C. Hilsum, S. Fray, and C. Smith, Solid State Commun. **7**, 1057 (1969).
[49] M. Lax, Phys. Rev. **119**, 1502 (1960).
[50] T. Sanada *et al.*, J. Phys. Soc. Jpn. **45**, N2, 501 (1977).